Inorg. Chem. **2007**, *46*, 8379–8390

Unpaired Spin Densities from NMR Shifts† and Magnetic Anisotropies of Pseudotetrahedral Cobalt(II) and Nickel(II) Vinamidine Bis(chelates)†

Rudolf Knorr,* Hermann Hauer, Alfons Weiss, Heinz Polzer, Friedrich Ruf, Peter Löw, Peter Dvortsák, and Petra Böhrer

Department of Chemistry and Biochemistry, Ludwig-Maximilians-Universität, Butenandtstr. 5−13, 81377 München, Germany

Received April 5, 2007

The distribution of unpaired electron spin over all regions of the organic ligands was extracted from the large positive and negative ^{1}H and ^{13}C NMR paramagnetic shifts of the title complexes. Owing to benevolent line broadening and to very high sensitivities of ≈254 000 and ≈201 000 ppm/(unpaired electron spin) for Co(II) and Ni(II), respectively, at 298 K in these pseudotetrahedral bis(*N*,*N*′-chelates), spin transmission through the σ- (and orthogonal π)-bonding system of the ligands could be traced from the chelate ring over five to nine σ bonds. Most of those "experimental" spin densities $\Delta\rho_N$ (situated at the observed nuclei) agree reasonably well with quantum chemical $\Delta\rho_{DFT}$ (DFT = density functional theory) values and provide an unsurpassed number of benchmark values for the quality of certain types of modern density functionals. The extraction of $\Delta\rho_N$ became possible through the unequivocal separation of the nuclear Fermi contact shift components from the metal-centered pseudocontact shifts, which are proportional to the anisotropy $\Delta\chi$ of the magnetic susceptibility: Experimental $\Delta\chi$ values were obtained in solution from measured deuterium quadrupole splittings in the ^{2}H NMR spectra of two deuterated model complexes and were found to be nonlinear functions of the reciprocal temperature. This provided the reliable basis for predicting metal-centered pseudocontact shifts for any position of a topologically well-defined ligand at varying temperatures. The related *ligand-centered* pseudocontact shifts were sought by using the criterion of their expected nonlinear dependence on the reciprocal temperature. However, their contributions could not be differentiated from other small effects close to the metal center; otherwise, they appeared to be smaller than the experimental uncertainties. The free activation energy of *N*-aryl rotation past a vicinal *tert*-butyl substituent in the Ni(II) vinamidine bis(*N*,*N*′-chelates) is $\Delta G^{\ddagger}$(+74 °C) ≈ 17.0 kcal/mol and past a vicinal methyl group $\Delta G^{\ddagger}$(−6 °C) ≈ 13.1 kcal/mol.

Introduction

Metal complexes of vinamidines (vinylogous amidines)[1] have received renewed attention during the past decade, for example as catalysts or because they can stabilize unusually low oxidation states by virtue of tunable shielding.[2] These six-membered ring bis(*N*,*N*′-chelates) **1** (Chart 1) are formed from two monovalent vinamidines on coordination to a divalent transition-metal cation (M^{2+}), with the four sp^2-hybridized nitrogen atoms in a pseudotetrahedral arrangement (if R^N > H)[2−4] which is known in detail from the crystal structures of **2**,[5] **3a**−**d**,[6] and further examples.[7−9] In formula **2** and later on, Ni/2 signifies that two identical vinamidine ligands are bound to Ni(II). Although the spiro-shaped, pseudotetrahedral complexes of type **1Co** and **1Ni** are

Chart 1

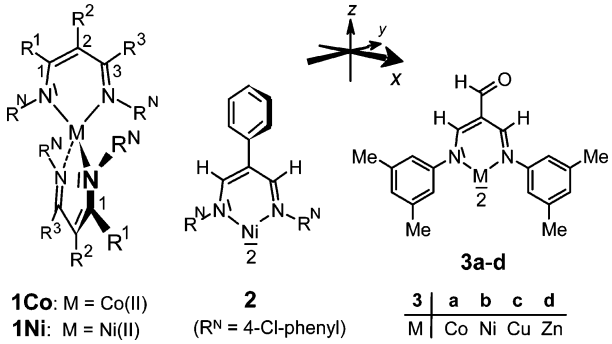

* To whom corresondence should be addressed. E-mail: rhk@cup.uni-muenchen.de.

† NMR of Paramagnetic Molecules, Part 15. For part 14, see ref 6.

(1) Lloyd, D.; McNab, H. *Angew. Chem.* **1976**, *88*, 496−504; Lloyd, D.; McNab, H. *Angew. Chem., Int. Ed. Engl.* **1976**, *15*, 459.

(2) Bourget-Merle, L.; Lappert, M. F.; Severn, J. R. *Chem. Rev.* **2002**, *102*, 3031−3065.

10.1021/ic700656r CCC: $37.00
Published on Web 09/01/2007

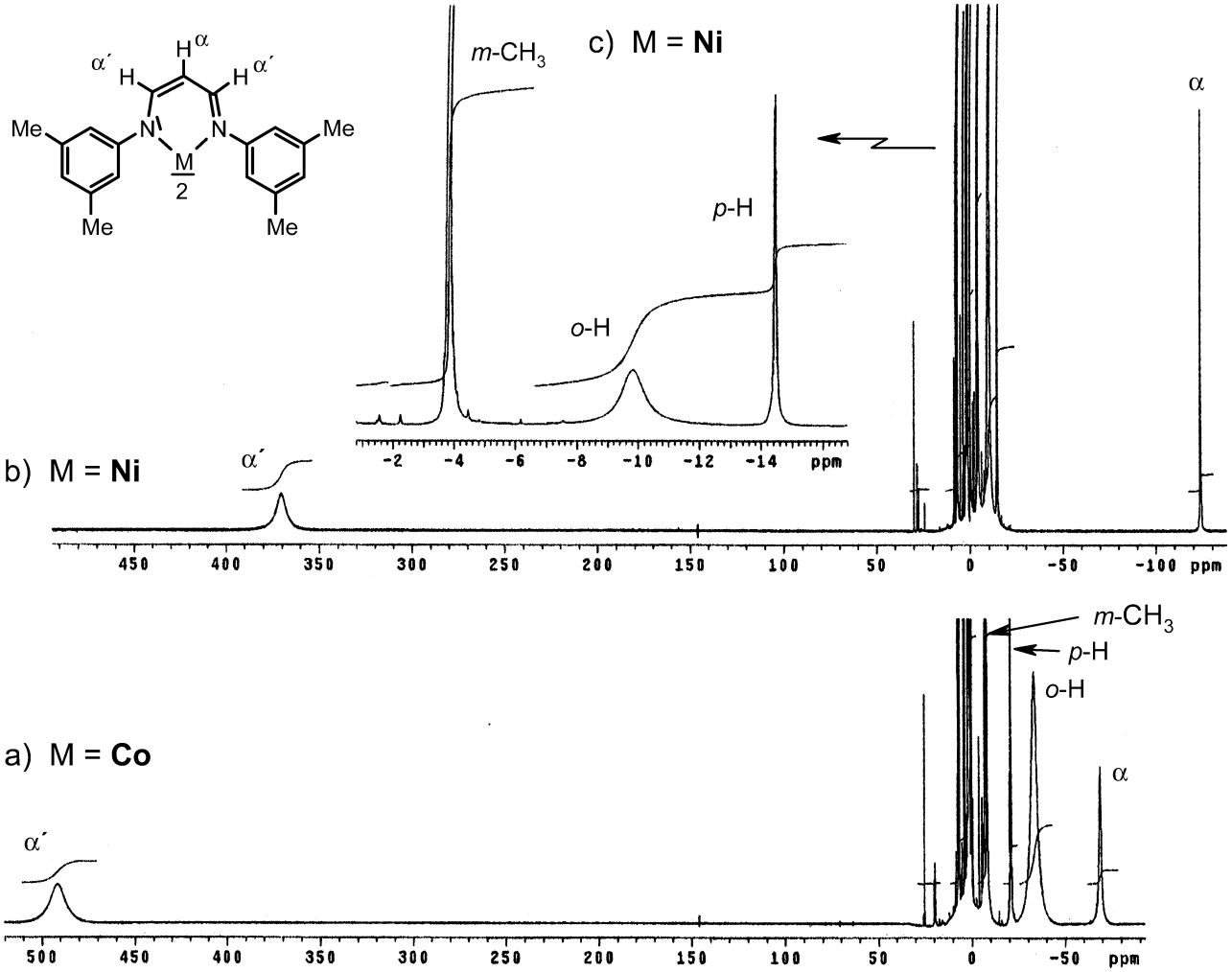

Figure 1. ^{1}H NMR spectra (400 MHz) of **6Co** (a) and **6Ni** (b and expansion c) at +19.5 °C in $CDCl_3$.

paramagnetic, their ^{1}H NMR absorptions are only moderately broadened, as shown for the cases of **6Co** and **6Ni** in Figure 1 where the chemical shifts of the chelate-ring protons (α and α′) can be seen to be more positive for Co(II) than for Ni(II), whereas the reverse is true for the *N*-aryl protons.

These unusually large positive and negative shift values and the even larger ^{13}C NMR shifts (exemplified in Figure 2) carry information about the interactions of unpaired electron spins with the ligand nuclei, but until now such information could not be analyzed in an unambiguous manner, as far as the shift-generating mechanisms could not be disentangled completely. The present work will demonstrate how to separate the through-bond from the through-space contributions by means of the known but rarely employed technique of nuclear quadrupole-induced ^{2}H NMR signal splitting, utilizing the deuterium-labeled examples **4Co** and **4Ni** (depicted in Chart 3). This technique can provide experimental values of the magnetic susceptibility anisotropies ($\Delta\chi$) in solution as the basis for calculating reliable through-space shift contributions in complexes having a well-defined geometry and little conformational flexibility. The through-bond contributions (δ^{CON}) will then be compared to the results of quantum chemical computations, with the aim of understanding the distribution of electron spin density over the organic ligands.

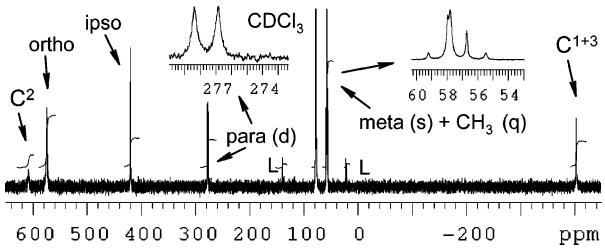

Figure 2. ^{13}C NMR spectrum (100.6 MHz, ^{1}H coupled) of **6Ni** (34 mg in $CDCl_3$, L = free ligand **6H**); structure displayed in Figure 1 or Chart 4. The insets show expansions of *p*-C (doublet, $^{1}J_{CH}$ = 155 Hz) and CH_3 (quartet, $^{1}J_{CH}$ = 125 Hz), the latter superposed on *m*-C (singlet). Accumulation of 141 440 transients at +27 °C, pulse width 15°, acquisition time 1.6 s, no delays.

(3) Lappert, M. F.; Liu, D.-S. *J. Organomet. Chem.* **1995**, *500*, 203−217.
(4) McGeachin, S. G. *Can. J. Chem.* **1968**, *46*, 1903−1912.
(5) Sheldrick, W. S.; Knorr, R.; Polzer, H. *Acta Crystallogr.* **1979**, *B35*, 739−741.
(6) Knorr, R.; Zölch, R.; Polborn, K. *Heterocycles* **1995**, *40*, 559−576.
(7) Dessy, G.; Fares, V. *Cryst. Struct. Commun.* **1979**, *8*, 101−106; *Chem. Abstr.* **1979**, *90*, 144552n.
(8) Healey, P. C.; Bendall, M. R.; Doddrell, D. M.; Skelton, B. W.; White, A. H. *Aust. J. Chem.* **1979**, *32*, 727−735.
(9) Further structures of type **1** may be gleaned from pp 3036, 3037, and 3043 of ref 2.

Pertinent Properties of the Complexes 1. The N_4 coordination (pseudo)tetrahedra are considerably elongated along the molecular *z* axis, as illustrated by the narrow endocyclic "bite" angles N−M−N = 97.3° for **3a** (M = Co)[6] and 94.7° for **3b** (Ni)[6] and 93.1° (averaged)[5] for **2** (Ni), 94.9° for **3c** (Cu),[6] and 97.4° for **3d** (Zn).[6] According to this elongation, the energetically degenerate pair of 3d orbitals of e (and π) symmetry at the transition-metal atom, d_{xz} and d_{yz}, is expected[10−12] to become higher in energy than d_{xy} and much higher than $d_{x^2-y^2}$ and d_{z^2} in the molecular $D_{2d}{}^z$ and $D_2{}^z$ symmetries. Consequently, the Ni(II) complexes **1Ni** have two of their eight 3d electrons with the spins unpaired in the e orbitals and hence are characterized by the total spin quantum number $S = 1$, whereas **1Ni** with R^N = H has a planar N_4 coordination sphere and is diamagnetic[3,4] ($S = 0$). Similarly, three electron spins are unpaired ($S = 1.5$) in the pseudotetrahedral **1Co** ($3d^7$) with the electron configuration $d_{xy}{}^1 d_{xz}{}^1 d_{yz}{}^1$. The resultant paramagnetism of **1Co** and **1Ni** can be described by an inversely temperature-dependent isotropic magnetic susceptibility χ in the Curie equation (eq 1), where μ is an effective magnetic moment (in units of the Bohr magneton $\mu_B = 0.92741 \times 10^{-23}$ J/T),[13a] $k = 1.38066 \times 10^{-23}$ J/K[13b] is the Boltzmann constant, and $\mu_o = 4\pi \times 10^{-7}$ henry/m[13c] is the vacuum magnetic permeability characteristic of the SI system[14−16] of physical units.

$$\chi = \mu^2 \mu_o (3kT)^{-1} \qquad (1)$$

By measurements of χ for numerous fully pseudotetrahedral bis(*N*,*N*′-chelates) in solution[17] and also in the solid state, we have found $\mu = 4.40$ (±0.30) μ_B for **1Co** and $\mu = 3.20$ (±0.20) μ_B for **1Ni** as the global averages. These data, which provided no strong indications of a temperature dependence of μ, confirmed the Curie-type ($1/T$) behavior of χ in eq 1, in accord with earlier reports[4,12,18−21] on closely related bis(chelates) **1**. The deviations of these μ data from the spin-only magnitudes[15] $\mu_{so} = 2\mu_B[S(S+1)]^{0.5}$ may be expressed by the rotationally averaged Landé splitting factors $g_{av} = \mu[S(S+1)]^{-0.5}/\mu_B$ as g_{av}(Co) = 2.27 (±0.15) and as (a fictitious)[22a] g_{av}(Ni) = 2.26 (±0.14). The corresponding paramagnetic susceptibilities[14,16] from eq 1 at 300 K are χ(Co) = 0.168 (±0.023) Å^3 and χ(Ni) = 0.089 (±0.011) Å^3 per molecule, or χ_M(Co) = 0.101 (±0.014) cm^3 mol^{-1} and χ_M(Ni) = 0.054 (±0.007) cm^3 mol^{-1}.

The pseudotetrahedral bis(chelates) **1** found in crystals are chiral (possessing C_2 or D_2 molecular symmetry but no mirror planes), as illustrated by the following nonorthogonal twist angles[5,6] between the two chelate planes: 88.6° for Co(II) in **3a** and 89.1° for Ni(II) in **3b** but 68.5° in **2**, 62.4° for Cu(II) in **3c**, and 88.5° for Zn(II) in **3d**. Ascent to the coplanar (0°) conformation of **1Ni** with R^N = aryl would require more than 23 kcal/mol.[23,24] Conversely, the spread of these interplanar angles (in particular of **3b** and **2**) indicates the potential surface of twisting to be flat toward the 90° conformation; at 90°, each of the two chelate rings would become a local mirror plane if $R^1 = R^3$, thus creating a $D_{2d}{}^z$ molecular symmetry if conformations or chirality of the substituents R^N and R^{1-3} are not taken into account. In the absence of crystal forces, this soft mode of torsion should become very active in solution (where typical examples of **1Co** and **1Ni** were always found[4,18,19] to be monomeric). Indeed, in all NMR spectra of **1** with $R^1 = R^3$ we observed the features of *effective* $D_{2d}{}^z$ symmetry alone, except for cases where slowly rotating substituents R^2 caused axial chirality.[23,25] Hence, the averaged effective susceptibility (χ) tensor of **1** may be expected to be *axially* symmetric, so that its anisotropy $\Delta\chi$ would be confined to the axially symmetric part $\Delta\chi = \chi_{zz} - (\chi_{yy} + \chi_{xx})/2$ (without a rhombic component). Knowledge of the magnitude of $\Delta\chi$ and of the orientation of its unique axis in solution is essential for analyzing the paramagnetically shifted NMR resonances of the bis(chelates) **1**, as outlined below.

Results and Discussions

The NMR Problem[26] of the Paramagnetic Bis(chelates) 1. Unpaired electron spin densities $\Delta\rho_N$ are the local differences[26] of electron densities with opposite spin directions. In accord with the quantum chemical formalism, $\Delta\rho_N$ is gauged in "atomic units" as the unpaired spin portion that resides in the volume element[27] $a_o{}^3 = 0.148185$ Å^3, which is centered *at the atomic nucleus* N.[28,29,30a,30b] As a contrast, the dimensionless *fractional population*[27,31a] $\Delta\rho_{BF}$ denotes the unpaired spin portion *in a basis function BF* (typically

(10) Lin, W. C.; Orgel, L. E. *Mol. Phys.* **1964**, *7*, 131−136. However, the assignment of a compressed (rather than elongated) bis(chelate) suggested therein was changed in ref 11a.
(11) (a) Eaton, D. R.; Phillips, W. D. *J. Chem. Phys.* **1965**, *43*, 392−398. (b) Ceulemans, A.; Dendooven, M.; Vanquickenborne, L. G. *Inorg. Chem.* **1985**, *24*, 1153−1158.
(12) Honeybourne, C. L.; Webb, G. A. *Mol. Phys.* **1969**, *17*, 17−31.
(13) (a) 1 joule/tesla = 10^3 erg/gauss. (b) 1 joule = 10^7 erg. (c) henry/m = $N \cdot A^{-2} = V\ s\ A^{-1}\ m^{-1}$.
(14) The χ values in this paper were calculated in the SI unit system.[15,16] For comparisons with older literature data, they may be converted to the now obsolete "irrational" (χ_{ir})[16] values in the cgs system by the relation $\chi = 4\pi\chi_{ir}$.
(15) Gerloch, M.; Constable, E. C. *Transition Metal Chemistry*; VCH: Weinheim, Germany, 1994.
(16) Mills, I.; Cvitaš, T.; Homann, K.-H.; Kallay, N.; Kuchitsu, K. *Quantities, Units and Symbols in Physical Chemistry*, 2nd ed.; Blackwell: Oxford, U.K., 1993. Homann, K.-H.; Hausmann, M. *Grössen, Einheiten und Symbole in der Physikalischen Chemie*, German ed.; VCH: Weinheim, Germany, 1996.
(17) Method described by Evans, D. F. *J. Chem. Soc.* **1959**, 2003−2005.
(18) Parks, J. E.; Holm, R. H. *Inorg. Chem.* **1968**, *7*, 1408−1416.
(19) Richards, C. P.; Webb, G. A. *J. Inorg. Nucl. Chem.* **1969**, *31*, 3459−3564.
(20) Bonnett, R.; Bradley, D. C.; Fisher, K. J.; Rendall, J. F. *J. Chem. Soc. A* **1971**, 1622−1627.
(21) Torgova, T. V.; Kurbatov, V. A.; Osipov, O. A. *Russ. J. Inorg. Chem.* **1981**, *26*, 63−65.
(22) McGarvey, B. R. *Inorg. Chem.* **1995**, *34*, 6000−6007. Specific reference details: (a) p 6005. (b) Figure 4 on p 6005. (c) Eq 2 on p 6000. (d) p 6004. (e) Figure 6 on p 6006. (f) Figure 5 on p 6005.
(23) Knorr, R.; Weiss, A.; Polzer, H.; Räpple, E. *J. Am. Chem. Soc.* **1977**, *99*, 650−651.
(24) Knorr, R.; Ruf, F. *J. Am. Chem. Soc.* **1979**, *101*, 5424−5425.
(25) Knorr, R.; Weiss, A.; Polzer, H. *Tetrahedron Lett.* **1977**, 459−462.
(26) Details are provided in the Supporting Information.
(27) Gerson, F. *Hochauflösende ESR Spektroskopie*; Verlag Chemie: Weinheim, Germany, 1967. Gerson, F. *High Resolution E.S.R. Spectroscopy*; Verlag Chemie: Weinheim, Germany, 1970.
(28) For the singly occupied 1s orbital of the free hydrogen atom as an example, $\Delta\rho_{1s} = 1$ but $\Delta\rho_N = |\psi_{1s}(0)|^2 = \pi^{-1}$ (au)$^{-1} = (\pi a_o{}^3)^{-1} = 6.748/\pi$ Å^{-3}. For other elements, see ref 30b or ref 29.
(29) Morton, J. R.; Preston, K. F. *J. Magn. Reson.* **1978**, *30*, 577−582.

of the characters BF = s, p, d, and so on). The through-bond "Fermi-contact" shift[26,32] δ^{CON} in eq 2 is caused by contact of the nuclear spin of N (^{1}H, ^{13}C) with $\Delta\rho_N$. As derived in the Supporting Information, eq 2 and all others were formulated here with strict observation of modern[14−16] physical units in order to compare the numerical findings with quantum chemical results.

$$\delta^{CON} = \mu_o g_{av}^{\ 2} \mu_B^{\ 2} (S+1)(9kTa_o^{\ 3})^{-1} \Delta\rho_N \qquad (2)$$

$$\vartheta^{CON} = \delta^{CON}\, T/(298\ \mathrm{K}) \qquad (3)$$

For analytical convenience, the experimental δ^{CON} values may be multiplied by T/(298 K) to provide the "reduced shifts" ϑ^{CON} in eq 3 which are reduced from a working temperature T to 298 K.[33,34] As far as the simple Curie-type ($1/T$) behavior (eq 2) applies, these ϑ^{CON} values are independent of the temperature and may be converted to spin densities through eqs 4a−c.

$$\Delta\rho_N = \vartheta^{CON}\,(298\ \mathrm{K}) 9ka_o^{\ 3} \mu_o^{\ -1} g_{av}^{\ -2} \mu_B^{\ -2} (S+1)^{-1} \qquad (4a)$$

$$\Delta\rho_N(\mathbf{1Co}) = 3.942\vartheta^{CON} \qquad (4b)$$

$$\Delta\rho_N(\mathbf{1Ni}) = 4.971\vartheta^{CON} \qquad (4c)$$

Although deviations from the Curie-type behavior may be expected,[30c,35a,35b] the theoretical Fermi contact parameters calculated[22b,26] for **1Co** and **1Ni** were proportional to $1/T$, thus establishing a necessary condition for computing spin densities via eq 2. Unfortunately, there are further components contributing to the experimental total NMR shifts[32] δ^{OBS} as denoted in eq 5. Of these, the isotropic paramagnetic NMR shift δ^{PARA} is obtained from δ^{OBS} by subtraction of the diamagnetic contribution δ^{DIA}, which can be measured at a constitutionally very similar but diamagnetic compound such as the zinc complex or (less accurately) the metal-free ligand.

$$\delta^{PARA} = \delta^{OBS} - \delta^{DIA} = \delta^{CON} + \delta^{MPC} + \delta^{LPC} \qquad (5)$$

$$\delta^{MPC} = \Delta\chi(12\pi)^{-1} G = \Delta\chi(12\pi)^{-1}(3\cos^2\theta - 1)R^{-3} \qquad (6)$$

Chart 2. Metal-Centered (a) and Ligand-Centered (b) Pseudocontact Interactions

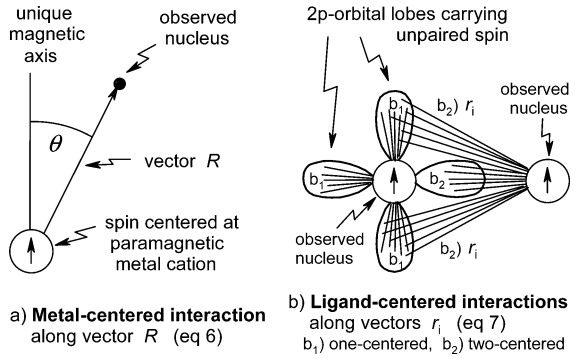

In the past, a serious obstacle to the experimental determination of spin densities from δ^{CON} values has consisted in the inadequate knowledge of the interfering through-space components δ^{MPC} and δ^{LPC} of δ^{PARA} in eq 5. Under axial magnetic symmetry, the *metal*-centered "*pseudocontact*" (MPC) contribution δ^{MPC} is proportional[14,32,36−38] to the susceptibility anisotropy $\Delta\chi$ according to eq 6 (where any second-order Zeeman contribution is contained[37b] in the measured $\Delta\chi$ value). This dipolar interaction[22c,30d,32,35c] of the electron spins (centered at the metal ion) with the nuclear spin under observation (situated at the ligand) *through space* depends on a geometry factor $G = (3\cos^2\theta - 1)R^{-3}$ which contains the angle θ spanned between the unique magnetic axis and the vector of length R connecting the metal center with the ligand nucleus, as shown in part a of Chart 2.

The *ligand*-centered *pseudocontact* (LPC) shift component δ^{LPC} comprises the pseudocontact (dipolar) coupling of a magnetically active ligand atom nucleus to the unpaired electron spin population $\Delta\rho_p$ residing in p-type atomic orbitals which are centered on this atom[30e,35d] (one-center model) or on its next neighbors[22d] (two-center interaction), as illustrated in part b of Chart 2. δ^{LPC} depends also on the local susceptibility anisotropy $\Delta\chi_L$ and on geometry factors[26] G_i^L in eq 7.

$$\delta^{LPC} = +\Delta\chi_L \sum_i [G_i^L (\Delta\rho_p)_i] \qquad (7)$$

As considered in the Supporting Information, $\Delta\chi_L$ and hence δ^{LPC} should be proportional to the sum $d_1/T + d_2/T^2$, so that the "reduced" contribution $\vartheta^{LPC} = \delta^{LPC}\, T/(298\ \mathrm{K})$ would depend on $1/T$. On this basis, we plan to detect δ^{LPC} shift "contaminations" of the contact shifts δ^{CON} in the following manner. After correction of the δ^{PARA} values (eq 5) for metal-centered pseudocontact shifts δ^{MPC} (eq 6), the remaining sum terms $\delta^{CON} + \delta^{LPC}$ will be multiplied by T/(298 K) to provide the "reduced shifts" $\vartheta^{C+L} = \vartheta^{CON} + \vartheta^{LPC}$. A *substantial* contamination by δ^{LPC} would then manifest itself by an additive term proportional to $1/T$ in the experimental sum ϑ^{C+L}. Other possible reasons for deviations

(30) *NMR of Paramagnetic Molecules*; La Mar, G. N., Horrocks, W. D., Holm, R. H., Eds.; Academic Press: NewYork 1973. Specific reference details: (a) p 95. (b) pp 558−559. (c) p 563. (d) Eq (1-53) on p 18 and eq (1-111) on p 39. (e) Eq (14-12) on p 562. (f) Eq (1-30) on p 11. (g) Eq (1-8) on p 6. (h) Eq (3-3) on p 86 and eq (3-17) on p 93. (i) p 88. (j) Eq (14A-6) on p 585.

(31) Carrington, A.; McLachlan, A. D. *Introduction to Magnetic Resonance*; Harper and Row: New York, 1967. Specific reference details: (a) p 81. (b) p 92. (c) p 82. (d) p 222.

(32) In contrast to the earlier usage[22,30,35] in NMR of paramagnetics, it is now customary to define the chemical shifts δ as positive in the *deshielded* (higher frequency) direction and to use SI units.

(33) This clear and simple means of searching for Curie-type behavior had been used in earlier work by: (a) Ho, F. F. L.; Reilly, C. N. *Anal. Chem.* **1969**, *41*, 1835−1841. (b) Golding, R. M. *Pure Appl. Chem.* **1972**, *32*, 123−135, in Table 1 therein.

(34) Knorr, R.; Polzer, H.; Bischler, E. *J. Am. Chem. Soc.* **1975**, *97*, 643−644.

(35) Kurland, R. J.; McGarvey, B. R. *J. Magn. Reson.* **1970**, *2*, 286−301. Specific reference details: (a) Eqs (40) and (42) on p 294. (b) Eq (50) on p 298. (c) Eq (17) on p 291. (d) Eq (53) on p 299. (e) Eqs (41) and (43) on p 294.

(36) McConnell, H. M. *J. Chem. Phys.* **1957**, *27*, 226−229.

(37) (a) Horrocks, W. DeW.; Fischer, R. H.; Hutchison, J. R.; La Mar, G. N. *J. Am. Chem. Soc.* **1966**, *88*, 2436−2442. (b) Horrocks, W. DeW. *Inorg. Chem.* **1970**, *9*, 690−692. (c) Horrocks, W. DeW.; Greenberg, E. S. *Biochim. Biophys. Acta* **1973**, *322*, 38−44.

(38) Banci, L.; Bertini, I.; Luchinat, C.; Pierattelli, R.; Shokhirev, N. V.; Walker, F. A. *J. Am. Chem. Soc.* **1998**, *120*, 8472−8479.

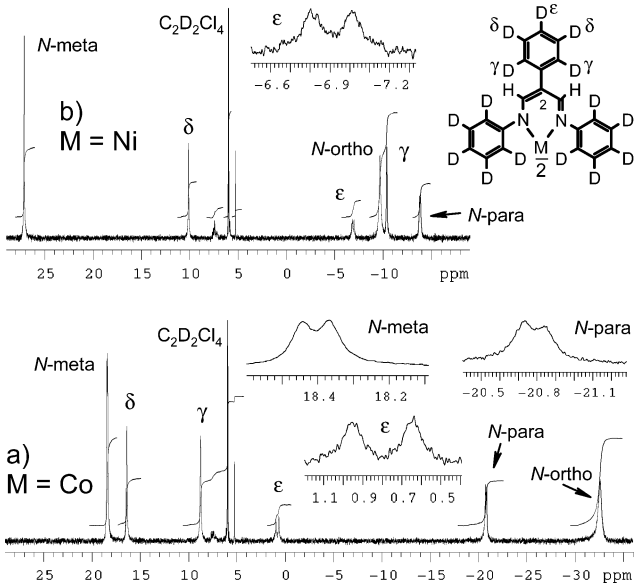

Figure 3. Deuterium NMR spectra (92.12 MHz) of **4Co** (a) and **4Ni** (b) at 300 K in CH_2Cl_2 with $Cl_2CD-CDCl_2$. The insets show the doublet splittings $\Delta\nu_D$ (induced by the deuterium nuclear quadrupole), which provided the magnitudes of the susceptiblity anisotropy.

from the Curie-type behavior will be treated as special effects, which have to be estimated or minimized in the planned investigations.

Magnetic Anisotropy and Metal-Centered Pseudocontact Shifts (δ^{MPC}). Very strong magnetic fields B_o can give rise to a slight molecular ordering in solution,[39] causing observable quadrupole splittings (1:1) of some deuterium (^2H = D) NMR signals, as shown in Figure 3 for the present type of complexes. The magnitudes of the frequency differences $|\Delta\nu_D|$ of this splitting depend on the susceptibility anisotropy, $\Delta\chi$, and on the angle ϕ between a C−D bond vector and the (as yet unknown) orientation of the unique magnetic axis. We used a simplified form[14,40,41] of this functional dependence, eq 8, as applicable to the deuterated bis(chelates) **4Co** and **4Ni** (Chart 3) with effective axial symmetry ($D_{2d}{}^z$). We employed $B_o = 14.1$ T together with the recommended[42] value of the nuclear quadrupole coupling constant $e^2qQ/h = 186.6$ (±6) kHz. The strong dependence of $|\Delta\nu_D|$ on $B_o{}^2$ and on the reciprocal temperature (roughly T^{-2} due to $\Delta\chi$) has been noticed already during the first applications[40,41] of this technique to paramagnetic octahedral Co(II) complexes.

$$|\Delta\nu_D| = (e^2qQ/h)B_o{}^2 \times |(3\cos^2\phi - 1)\Delta\chi| \times (20\mu_o kT)^{-1} \quad (8)$$

The complexes[43] **4Co** and **4Ni** were chosen because they were thought to have little conformational flexibility other

Chart 3

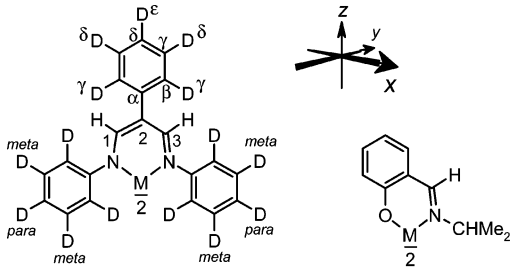

4H: M/2 = H **4Ni**: M = Ni **5Co**: M = Co
4Co: M = Co **4Zn**: M = Zn **5Ni**: M = Ni

than phenyl rotation. The δ^{OBS} values of D^γ, D^δ, and D^ϵ and of the deuterium atoms at the *N*-phenyl groups (*N*-*o*-D, *N*-*m*-D, *N*-*p*-D) agreed with those in the published ^1H NMR spectra where all assignments are known.[44] The unknown parameters in eq 8 are $\Delta\chi$ and the angles ϕ. The largest splittings $|\Delta\nu_D|$ at a certain temperature in Table 1 belong to D^ϵ of **4Co** and **4Ni**. This immediately suggests that the unique magnetic axis might be oriented nearly parallel to the $C^\delta-D^\epsilon$ bond vector in **4**, because $3\cos^2\phi - 1$ of eq 8 will be at maximum when $\phi = 0$; indeed, a numerical analysis[26] confirms the coincidence of the magnetic with the *z* ($C^\delta-D^\epsilon$) axis. On this basis, the molecular $\Delta\chi$ and molar $\Delta\chi_M$ values[14] (Table 1) have been computed from measured $|\Delta\nu_D\ (3\cos^2\phi - 1)^{-1}|$ data via eq 8. The signs of $\Delta\chi$ do not follow from the experiments but were chosen to be in accord with the explicit model calculations[22e] and with the single-crystal susceptibilities[45,46] of the related complexes **5Co** and **5Ni**. These single-crystal values translate, after multiplication[14] by 4π, to $10^6\Delta\chi_M$(**5Co**) = +43 165 cm^3 mol^{-1} (at 298 K)[46] and $10^6\Delta\chi_M$(**5Ni**) = −27 835 cm^3 mol^{-1} (at 300 K)[45b] or 176% (Co) and 169% (Ni) of our $\Delta\chi_M$ values in Table 1, as might have been anticipated in view of the lower symmetry of **5Co** and **5Ni**. Although $\Delta\chi$ is the sum of the paramagnetic and diamagnetic anisotropies, it was found that the diamagnetic part could be neglected here because it was too small to give observable NMR splittings $|\Delta\nu_D|$ of the diamagnetic Zn(II) complex **4Zn**.

The temperature dependence of $\Delta\chi$ in Table 1 is stronger than $1/T$ (Curie), so the product $T\Delta\chi$ is not constant but can be fitted (see Figure S5, Supporting Information)[26] to an additive term which is proportional to $1/T$, corresponding to the T^{-2} terms in eqs 9a,b. The functional form ($m_1/T + m_2/T^2$) of eqs 9 and 10a was chosen to agree with that obtained[14,47] from the explicit model calculations[22e] on **1Co** and **1Ni**, in keeping with the general δ^{MPC} theory.[35e] However, the theoretical[22e] anisotropy values at 298 K (namely, $10^3\Delta\chi$(Co,calcd) = +22.6 Å^3 and $10^3\Delta\chi$(Ni,calcd)

(39) van Zijl, P. C. M.; Ruessink, B. H.; Bulthuis, J.; MacLean, C. *Acc. Chem. Res.* **1984**, *17*, 172−180 and cited refs.
(40) Domaille, P. J. *J. Am. Chem. Soc.* **1980**, *102*, 5392−5393.
(41) Domaille, P. J.; Harlow, R. L.; Ittel, S. D.; Peet, W. G. *Inorg. Chem.* **1983**, *22*, 3944−3952.
(42) Bestiaan, E. W.; MacLean, C.; van Zijl, P. C. M.; Bothner-By, A. A. *Ann. Rep. NMR Spectrosc.* **1987**, *19*, 35−77, on p 65.
(43) Greek labels for the substituent atoms refer to the number of bond distances from chelate position 2, from which C^α and C^β are one and two bonds away, respectively, C^γ and D^γ are three bonds away, and so on. Similarly, α', *β*', and *γ*' count the distances from chelate positions 1 and 3.
(44) Knorr, R.; Weiss, A.; Polzer, H.; Bischler, E. *J. Am. Chem. Soc.* **1975**, *97*, 644−646.
(45) (a) Gerloch, M.; Slade, R. C. *J. Chem. Soc. A* **1969**, 1022−1028. (b) Cruse, D. A.; Gerloch, M. *J. Chem. Soc., Dalton Trans.* **1977**, 152−159.
(46) Horrocks, W. DeW.; Burlone, D. A. *Inorg. Chim. Acta* **1979**, *35*, 165−175. These authors used the solid-state anisotropies of **5Co** and **5Ni** for separating the Fermi contact from the pseudocontact components.
(47) Analyzed from enlarged versions of the diagrams in ref 22 as obtained through the courtesy of Prof. B. R. McGarvey.

Table 1. Deuterium NMR Resonance Splitting $|\Delta\nu_D|$ and Magnetic Anisotropies (Molecular, $\Delta\chi$, and Molar, $\Delta\chi_M$) of the Paramagnetic Susceptibilities of the Bis(chelates) **4Co** and **4Ni** in CH_2Cl_2 Solution as a Function of the Temperature

		$\|\Delta\nu_D\|$ [Hz]						
complex	T [K]	D$^{\epsilon}$	D$^{\delta}$	D$^{\gamma}$	*N*-*p*-D	*N*-*m*-D	$10^3\Delta\chi$ [Å^3]	$10^6\Delta\chi_M$ [cm^3 mol^{-1}]
4Co	300	29.0 ± 0.5	< 5	< 5	11.0 ± 0.5	7.2 ± 0.3	(+)40.7 ± 0.7	(+)24510 ± 420
	285	32.0 ± 0.5	< 5	< 5	12.5 ± 0.5	8.0 ± 0.3	(+)42.7 ± 0.7	(+)25684 ± 400
	270	36.5 ± 0.5	< 6	< 6	< 16	9.5 ± 0.4	(+)46.1 ± 0.6	(+)27755 ± 380
	250	44.0 ± 1.0	< 10	< 10	< 18	11.4 ± 0.6	(+)51.4 ± 1.2	(+)30983 ± 700
	230	53.0 ± 2.0	< 19	< 19	< 29	< 16	(+)57.0 ± 2.2	(+)34331 ± 1300
4Ni	300	19.5 ± 0.5		< 3	8.0 ± 0.5		(−)27.4 ± 0.7	(−)16500 ± 420
	270	25.0 ± 0.5	< 6	< 6	<14	< 7	(−)31.6 ± 0.6	(−)19011 ± 380
	250	30.0 ± 1.0	< 7	< 7	< 18	< 8	(−)35.1 ± 1.2	(−)21125 ± 700
	230	35.0 ± 4.0	< 15	< 13	< 25	< 12	(−)37.3 ± 4.3	(−)22673 ± 2600

= −44.3 Å^3)[48] were 55% (Co) and 164% (Ni) of our experimental values at 300 K in Table 1. Thus, the calculated quotient −0.50 for Co/Ni was much smaller than the experimental quotients of −1.48 for **4Co**/**4Ni** and −1.58 for **5Co**/**5Ni**. The suspicion that the calculations[22] were of better quality for Co(II) than for Ni(II) was fostered by analyses[47] of the calculated[22e] $\Delta\chi_{ir}/3$ values ("ir" = "irrational")[14] in which the T^{-2} term contributed 20% for Co and 10% for Ni at 298 K, whereas the experimental contributions of T^{-2} determined here at 300 K (eqs 9a,b and Figure S5, Supporting Information) are 21.5% for both Co and Ni.

$$\Delta\chi(\text{Co}) = +9.6\ \text{K}\cdot\text{Å}^3/T + 778.0\ \text{K}^2\cdot\text{Å}^3/T^2 \qquad (9a)$$

$$\Delta\chi(\text{Ni}) = -6.5\ \text{K}\cdot\text{Å}^3/T - 533.0\ \text{K}^2\cdot\text{Å}^3/T^2 \qquad (9b)$$

$$\delta^{\text{MPC}} = (m_1/T + m_2/T^2)(3\cos^2\theta - 1)R^{-3} \qquad (10a)$$

$$m_1(\text{Co}) = +0.2546\ \text{K}\cdot\text{Å}^3 \text{ and } m_2(\text{Co}) = +20.64\ \text{K}^2\cdot\text{Å}^3 \qquad (10b)$$

$$m_1(\text{Ni}) = -0.1724\ \text{K}\cdot\text{Å}^3 \text{ and } m_2(\text{Ni}) = -14.14\ \text{K}^2\cdot\text{Å}^3 \qquad (10c)$$

The eqs 10a−c, derived from eqs 9a,b in combination with eq 6, allow one to compute the metal-centered pseudocontact shifts δ^{MPC} for other experimental temperatures, provided that the polar coordinates θ and R can be estimated. For this purpose, the chelate parts of **1Co** and **1Ni** were measured in their averaged natural geometries as taken from the solid-state structures[5,6] of **2**, **3a**, and **3b**. However, the spiroheterocyclic twist angle was fixed at 90° (local $D_{2d}{}^z$ symmetry, ignoring substituent conformations), and all hydrogen atoms (C−H = 1.09 Å) and the carbon atoms of substituents at the N atoms and at C^{1,3} and C^2 were placed at their idealized positions for the topological analyses. Nuclei positioned close to the z axes in **1** and **4** ($\theta \approx 0$) will have positive (deshielded) δ^{MPC} values if M = Co, but negative (shielded) δ^{MPC} values if M = Ni. Table S2 (Supporting Information) specifies the polar coordinates θ and R of eqs 6 or 10a together with the G factors computed therefrom.[26]

Nuclei rotating about the molecular z axis (C^2−R$^{\alpha}$ in Chart 4) do not change their θ and R values (assuming rigid rotation), and nuclei residing in or at the para position of the *N*-aryl groups also have practically rotation-independent polar coordinates. For all other nuclei, the geometry factors $G = (3\cos^2\theta - 1)R^{-3}$ had to be averaged over the relevant conformations.[26] For nuclei other than C^{1,3} and C^2, δ^{MPC} at 298 K can be seen in Table S2 (Supporting Information) to span the ranges from +27.0 (H$^{\alpha}$) to −30.1 ppm (*N*-*ipso*-C) for Co(II) and from −17.8 (H$^{\alpha}$) to +21.7 ppm (*N*-*ipso*-C) for Ni(II). The magnitude of δ^{MPC}(Ni) drops to below 1 ppm for the ϑ and ι (iota) positions (entries S2.95 and S2.96 of Table S2) over a distance of eight and nine bonds, respectively, from the chelate ring in **28** (Chart 4).

The numerous bis(chelates) depicted in Chart 4[43] were chosen not only to provide a broad basis of examples with limited conformational flexibility but many of them were also needed to achieve unambiguous NMR assignments through comparisons of related structures, because the scalar interproton (Figure 1) and $^{13}C-^{1}H$ splittings were usually not resolved due to paramagnetic line broadening. Exceptions are shown in Figure 2 for **6Ni** where two one-bond C−H splittings $^1J_{CH}$ were detected and served to assign the resonances whose ^{13}C signal integrations did not allow a conclusive decision: *p*-C (C−H doublet) was distinguished from *ipso*-C (singlet), and the assignment of nearly coinciding shifts (at ≈ +58 ppm) of four *m*-C (singlet) and four CH_3 (C−H quartet) was established. Assignments through methyl substitution provided the additional bonus of differentiating[26] σ and π spin transmission.

Ligand-Centered Pseudocontact Shifts (δ^{LPC}). This contribution (eq 7) should be proportional to $(d_1/T + d_2/T^2)$, as suggested by explicit calculations[22f] (eq S7a, Supporting Information).[26] In a search of this $1/T^2$ attribute, which was encouraged by the existence of other $1/T^2$ models,[49,50] the sums $\vartheta^{\text{C+L}}$ of "reduced" shifts were plotted against $1/T$ in Figures S1−S4 (Supporting Information) where the line numbers refer to nuclei which are listed in Table S1 (Supporting Information). Deviations from the horizontal course should be proportional to $1/T$ if caused by an admixture of $\vartheta^{\text{LPC}} = \delta^{\text{LPC}}\,T/(298\ \text{K}) = (d_1 + d_2/T)(298\ \text{K})^{-1}\sum_i[G_i^{\text{L}}(\Delta\rho_p)_i]$, with the slopes depending on the p-orbital spin populations $(\Delta\rho_p)_i$. A distinct hint at this cause was encountered for $\vartheta^{\text{C+L}}$ of C^{1,3} (lines 27−31 in Figure S1), probably owing to the very large $\Delta\rho_p$ values at each nitrogen atom in combination with a favorable, almost complete z alignment of the N−C^1 (and N−C^3) bond vector, which

(48) Converted from the calculated "DP" = $\Delta\chi_{ir}/3$ values in Table 1 of ref 22 through multiplication[14] by the factor $12\pi \times 10^{24}$.

(49) Mispelter, J.; Momenteau, M.; Lhoste, J.-M. *J. Chem. Soc., Dalton Trans.* **1981**, 1729−1734, on p 1731.

(50) Acerete, R.; Casañ-Pastor, N.; Bas-Serra, J.; Baker, L. C. W. *J. Am. Chem. Soc.* **1989**, *111*, 6049−6056.

Chart 4. Vinamidines and Their Bis(chelate) M(II) Complexes, with Positional Numbering[43] as Used in the Tables (d = distant and n = near)

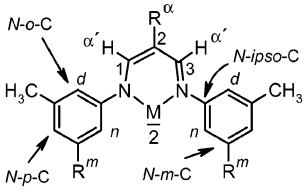

	M/2	R^{α}	R^{m}
6H	H	H	CH_3
6Co	Co	H	CH_3
6Ni	Ni	H	CH_3
6Cu	Cu	H	CH_3
7H	H	H	H
7Ni	Ni	H	H
8H	H	Ph	H
8Ni	Ni	Ph	H

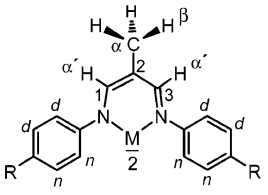

	M/2	R
9H	H	H
9Ni	Ni	H
10H	H	CH_3
10Co	Co	CH_3
10Ni	Ni	CH_3
10Zn	Zn	CH_3

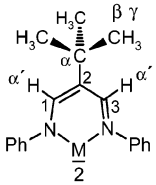

11H: M/2 = H
11Co: M/2 = Co
11Ni: M/2 = Ni

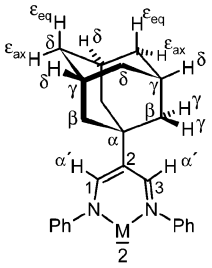

12H: M/2 = H
12Co: M/2 = Co
12Ni: M/2 = Ni

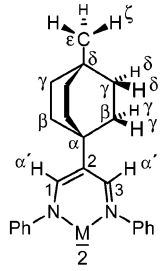

13H: M/2 = H
13Co: M/2 = Co
13Ni: M/2 = Ni

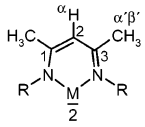

	M/2	R
14H	H	CH_3
14Ni	Ni	CH_3
15H	H	Ph
15Co	Co	Ph
15Ni	Ni	Ph
16H	H	3,5-$Me_2C_6H_3$
16Ni	Ni	3,5-$Me_2C_6H_3$
17Ni	Ni	3-MeC_6H_4
18Ni	Ni	2-MeC_6H_4

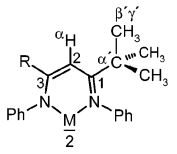

	M/2	R
19H	H	*tert*-butyl
19Co	Co	*tert*-butyl
19Ni	Ni	*tert*-butyl
20H	H	H
20Ni	Ni	H
20Zn	Zn	H

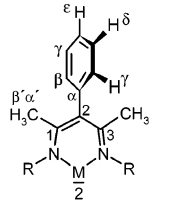

	M/2	R
21H	H	CH_3
21Ni	Ni	CH_3
22H	H	3,5-$Me_2C_6H_3$
22Ni	Ni	3,5-$Me_2C_6H_3$
23H	H	Ph
23Ni	Ni	Ph

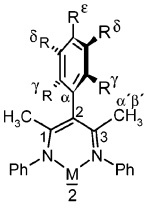

	M/2	R^{γ}	R^{δ}	R^{ε}
24H	H	H	H	CH_3
24Ni	Ni	H	H	CH_3
25H	H	CH_3	H	CH_3
25Ni	Ni	CH_3	H	CH_3
26H	H	H	CH_3	H
26Ni	Ni	H	CH_3	H
27H	H	CH_3	CH_3	H
27Ni	Ni	CH_3	CH_3	H

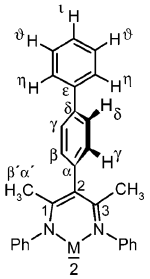

28H: M/2 = H
28Ni: M/2 = Ni

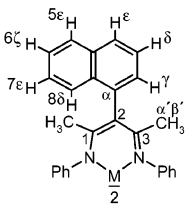

29H: M/2 = H
29Ni: M/2 = Ni

implies a close to maximum interaction in the ($3\cos^2\phi - 1$) model[22d] of the geometry factor G_i^{L}. The appertaining slopes of lines 27−31 are specified in the footnotes of Table S1, but an interpretation is not attempted here because of the multitude of possible interactions, in keeping with a recommendation[51] to use empirical ϑ^{LPC} estimates. Extrapolation to $1/T = 0$ would eliminate merely the hyper-Curie[38] portion of ϑ^{LPC}, but this portion might be overestimated to an unknown extent, because its slope could also be attributed to a temperature-dependent spin density $\Delta\rho_N$ in the reduced contact shift ϑ^{CON} (eq 2 with eq 3) in the case[52,53] of an excessive thermal excitation of nuclear displacements. For example, for $C^{1,3}$, such displacements would entail ϑ^{CON} changes going in the same direction as the suspected ϑ^{LPC} (to be shown in the supplementary[26] density functional theory (DFT) section). Thus it would appear inadvisable to rely too heavily on the numerical details of the conjectured $1/T^2$ dependence of $\Delta\chi_L$ in the chosen model.[51,54] Hence, the additional (Curie-type) portion of ϑ^{LPC} was left in a sum ϑ^{C+L} together with ϑ^{CON}, and its estimation and final elimination was not attempted, so that the magnitude of $\vartheta^{CON} \approx \vartheta^{C+L}$ denoted for $C^{1,3}$ may still be too large (by probably less than 4−11%).

Presumably owing to substantially smaller $(\Delta\rho_p)_i$ densities or to the mutual cancellation of their effects and/or to unfavorable G_i^{L} factors, most of the other correlation lines for rotationally indifferent nuclei in Figures S1−S4 (Supporting Information) appear to run with practically zero slope. Exceptions are provided by the rotation-sensitive protons of the 2-phenyl[44] substituent in **8Ni** (lines 38, 41, and 42 in Figure S2), by a few of the nuclei in the *N*-aryl groups (lines 13, 14, 22, 43, 44, 78, and 80−83), and by $H^{8\delta}$ (= *peri*-H) of **29Ni** (line 33, to be discussed at the end of the Supporting Information computational section as a possible effect of ϑ^{LPC}).

Reduced Contact Shifts ϑ^{CON} and "Experimental" Spin Densities $\Delta\rho_N$. An inspection of Table S1 (Supporting Information) reveals that the magnitudes $|\Delta\rho_N|$ for corresponding nuclei tend to be smaller in the Co(II) than in the isostructural Ni(II) bis(chelates). As an exception, the actual $\Delta\rho_N$ difference is tiny for $H^{\alpha'}$ (Chart 4) whose strongly positive ϑ^{CON}(**6Co**) = +449 (entry S1.88) and ϑ^{CON}(**6Ni**) = +363 (line 7; entry S1.92)[55] translate to almost the same $\Delta\rho_N$ value of ≈+0.00179. This rather large $\Delta\rho_N$ value may be attributed partly to σ-bond interactions along the generally favorable anti coupling path, namely, cation−*N*−C^1−$H^{\alpha'}$. The same anti route seems to develop twice as much spin density (roughly +0.0034) at $C^{\alpha'}$ (methyl carbon) in both **15Co** and **15Ni** (S1.84 and S1.86). In another type of interaction, each of the two chelate ligands can donate a small fraction (for example, $^1/_{13}$ electron)[18] of its negative π spin

(51) Mispelter, J.; Momenteau, M.; Lhoste, J. M. *Biol. Magn. Reson.* **1993**, *12*, 299−355.
(52) Eicher, H.; Köhler, F. H.; Cao, R. *J. Chem. Phys.* **1987**, *86*, 1829−1835, on pp 1829 and 1833.
(53) Eicher, H.; Köhler, F. H. *Chem. Phys.* **1988**, *128*, 297−309, on p 307.
(54) Eq 8 of ref 38.
(55) This value deviates strongly from $\delta^{PARA} = +51$ as reported[32] in ref 18 for the scarcely soluble analogue of **6Ni** devoid of all methyl groups.

Chart 5

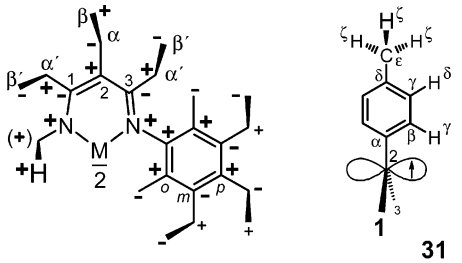

30 ($\Delta\rho_N$) **31** (part of **24Ni**)

density into the cation's half-filled orbitals (d_{xz} and d_{yz}), leaving net positive π spin density on the ligand. Thus the ligand's 6π electron system develops the down-scaled spin density pattern[18,56] of a 1,5-diaza-2,4-pentadienyl π radical, $+ - + - +$, positive at C^2 and the two nitrogens but negative (by π-electron correlation)[31b] at C^1 and C^3. This induces large positive $\Delta\rho_N$ and ϑ^{CON} values at C^2 (entries S1.6−S1.9; lines 1 and 3) but entails, by sign-reversing π/σ spin polarization,[31c,57] typically much smaller *negative* spin densities at H^α (S1.106−S1.110; lines 23, 62, and 63) and twice as negative ones at C^α of the Co(II) and Ni(II) bis(chelates) (S1.103−S1.105; lines 25 and 26). Similarly, *N*-*o*-H (lines 20, 57, and 83; S1.27−S1.33), *N*-*p*-H (lines 77−82; S1.62−S1.74), and *N*-*p*-CH_3 (line 21; S1.81 and S1.82) owe their smaller negative $\Delta\rho_N$ partly to sign-reversing π/σ spin polarization by positive $\Delta\rho_N$ values at their next neighbors. *N*-*m*-H (lines 18, 55, and 69; S1.43−S1.50) and *N*-*m*-CH_3 (line 17; S1.75 and S1.76) get their smaller positive $\Delta\rho_N$ values partly through negative $\Delta\rho_N$ at *N*-*m*-C in a corresponding manner, whereas *N*-*i*-C (lines 47−49 and 53; S1.11−S1.19) is the single exception to the sign inversion (Chart 5). Stepping one bond ahead from C^α toward C^β and H^β leads to another sign reversal (S1.111−S1.116; lines 8, 11, 12, 15, and 16), but these positive spin densities are too large to be caused by spin polarization from C^α alone; rather they are attributable mainly to spin transfer (with sign retention) by the direct orbital overlap between the $C^\alpha-C^\beta$ or $C^\alpha-H^\beta$ bonds and the chelate π system. These latter interactions ("hyperconjugation") become possible when the β atoms are not fixed in the nodal plane of the π system, and they explain also the diverse signs of $\Delta\rho_N$ at $H^{\beta'}$ (lines 58 and 59; S1.95−S1.99), *N*-*m*-CH_3 (lines 39, 40, and 76; S1.77−S1.80), and *N*-*p*-CH_3 (S1.83; line 54). The more detailed analyses[26] rely on the technique of methyl substitution.

The sketch **30** in Chart 5 illustrates the measured ρ_N sign pattern (not always equal to the $\Delta\rho_\pi$ sign pattern of the sp^2 centers) for both Co(II) and Ni(II) bis(chelates), with the reservation that the shifts of C^2 and $C^{1,3}$ and of *N*-methyl protons could not be observed in Co(II) complexes and that *N*-*p*-CH_3 (entry S1.83; line 54) was studied for **10Co** only. The arrangement of the substituents in **30** does not belong to one real compound, of course; rather it illustrates that, for example on the left of **30**, ϑ^{CON} of *N*−CH_3 (entry S1.10; line 9) in **14Ni** and **21Ni** is strongly positive. By virtue of the hyperconjugation mechanism, this allows the backward conclusion that the nitrogen atoms carry strongly positive π spin density, evidence which could not be obtained by direct measurement.

Table 2. Reduced Fermi Contact Shifts $\vartheta^{CON} \approx \vartheta^{C+L}$ Caused by Transmission of Unpaired Spin Density through sp^3 Centers in 2-(4-Methyl-1-bicyclo[2.2.2]octyl) Substituents (**13Co**, **13Ni**) and through sp^2 Centers in Nonconjugated 2-Aryl Groups (**24Ni**, **28Ni**)

	ϑ^{CON} of compound no.			
nucleus	**13Co**	**13Ni**	**24Ni**	**28Ni**
C^2		+690	+670	
C^α	−224	−227	−263	
C^β	+168	+174	+305	
C^γ	+20.0	+20.0	+22.8	
H^γ	−3.7	−1.6	−2.4	−2.4
C^δ	−1.3	−2.47	+8.5	
H^δ	+1.0	+1.95	+4.0	+4.48
C^ϵ	+0.85	−1.3	−3.9	
H^ζ	−0.10	+0.18	+2.1[a]	[b]

[a] Value of +0.93 ppm for **25Ni** in entry S1.162 of Table S1 (Supporting Information). [b] H^η, +0.46 ppm; H^ϑ, +0.53 ppm; H^ι, −0.08 ppm.

The source of π spin density at chelate center C^2, as diagnosed separately,[26] can induce $\Delta\rho_N$ with alternating signs in a conjugated 2-phenyl substituent, as shown by ϑ^{CON} = −10.5 (H^γ, ortho, line 41), +5.6 (H^δ, meta, line 32), and −12.0 (H^ϵ, para, line 42) of **8Ni** (entries S1.129, S1.139, and S1.157, respectively, in Table S1, Supporting Information).[58] Such π delocalization depends on the $\cos^2$ of the interplanar angle between 2-phenyl and the chelate ring, so that these delocalized spin densities decrease with increasing temperature.[44] To get rid of this complicating π mode, flanking 1,3-methyl substituents in **21**−**29** were used to lock the 2-aryl groups in a nearly perpendicular conformation that is sketched in **31** and thwarts π conjugation (because $\cos^2 90° = 0$). For a para proton (H^ϵ in line 37; entry S1.155), ϑ^{CON} has dropped then to −1.2 ppm; for H^ζ of the *p*-CH_3 group, the small ϑ^{CON} = +2.1 (entry S1.161) of **24Ni** is reduced to ϑ^{CON} = +0.93 (line 56; S1.162) in the mesityl substituent of **25Ni**. Table 2 collates some of these and several further ϑ^{CON} values of **24Ni** along with those of the biphenylyl derivative **28Ni** and the saturated 1-bicyclo[2.2.2]-octyl substituents in **13Co** and **13Ni**. The strikingly large positive value of ϑ^{CON} = +305 of $^{13}C^\beta$ in **24Ni** (entry S1.114; line 8) can be understood through $\pi-C^\beta$ hyperconjugation, which is at its maximum in the perpendicular conformation **31**. Several ^{13}C NMR contact shifts of **13Co** and **13Ni** resemble those of **24Ni**, but ϑ^{CON} = +174 of C^β (S1.113; line 11) in **13Ni** is roughly one-half of that in **24Ni** because of the expectation value $\langle\cos^2\alpha\rangle = 0.5$ for the angular factor of $\pi-C^\beta$ hyperconjugation (see **31**) under conditions of free rotation of the bicyclic 2-substituent in **13Ni**. The favorable W-shaped σ-bond pathway from C^2 to (*m*-)H^δ may be a reason for the unexpectedly large ϑ^{CON} values of +4.0 of H^δ in **24Ni** (S1.141) and +4.48 in **28Ni** (line 19; S1.140 or Table 2) and +5.6 in **25Ni** (line 32; S1.139); any π contribu-

(56) Honeybourne, C. L. *Chem. Phys. Lett.* **1971**, *8*, 493−496.
(57) McConnell, H. M.; Chesnut, D. B. *J. Chem. Phys.* **1958**, *28*, 107−117 and cited refs.
(58) The ϑ^{CON} values given for **8Ni** differ from those in ref 44 by sign reversal[32] and also in their magnitudes, because that preliminary publication[44] dealt with $-\vartheta^{PARA}$ values which could not yet be corrected for ϑ^{MPC} at that time.

tion should be small in **24Ni**−**27Ni** according to the criteria[26] of methyl substitution. Furthermore, the phenyl group at C^{δ} (Charts 4 and 5) of **28Ni** possesses undisturbed biphenyl π conjugation: it should exhibit alternating signs of its ϑ^{CON} values (as exemplified above for **8Ni**) if there was perceptible unpaired π spin density present at its anchor position C^{δ}. Instead, ϑ^{CON} is small and positive for both H^{η} and H^{ϑ} (entries S1.165 and S1.166). This indicates that non-π effects dominate the spin transmission through these chains of sp^2 centers along up to nine σ bonds (up to H^{ι}) away from C^2. The second and third columns of Table 2 provide comparisons with spin transmission through sp^3 centers, which terminates already at five (admittedly somewhat longer) σ bonds away from C^2, as shown for H^{ζ} of **13Co** and **13Ni**.

Computed Spin Densities $\Delta\rho_{DFT}$. Quantum chemical computation using the recommended[26,59,60] technique of DFT, as implemented in the *Gaussian* program[61] packages, is a good means of validating a basic assumption made in the Introduction: The computational variation of the bis(chelate) interplanar twist angle from 90° (perpendicular chelate planes) down to 60° produced only modest changes of the magnitudes $|\Delta\rho_{DFT}|$ for most of the *peripheral* nuclei (Table S3a, Supporting Information, entry S3a.8 versus S3a.6 and entry S3a.16 vs S3a.14). Therefore, the 90° twist structure, which had been adopted as a suitable model for the torsional averaging of both calculated and experimental spin densities, appeared to be a reasonable choice and was used in producing the $\Delta\rho_{DFT}$ data listed in Table S1 (Supporting Information). It may be noticed that the magnitudes of both $\Delta\rho_{DFT}$ and $\Delta\rho_N$ in Table S1 tend to be smaller for Co(II) than for the isostructural Ni(II) complexes, even though the corresponding ϑ^{CON} values may be practically equal (entries S1.11 ≈ S1.15, S1.106 ≈ S1.109, S1.111 ≈ S1.113).

A general first impression from Table S1 suggests that the computed $\Delta\rho_{DFT}$ magnitudes are very often appreciably larger than the appertaining "experimental" $\Delta\rho_N$ data: The plot of $\Delta\rho_{DFT}$ against $\Delta\rho_N$ in Figure 4 calls for a slightly larger slope than displayed by the 1:1 correlation line, even with the best-suited basis set 6-311G(d,p) under the UB3LYP method. Because most of the experimental ϑ^{CON} data appear to be well established, with uncertainties below the 10% level (at least for the geometrically fixed or the rotationally *z*-symmetric groups of nuclei), the problem might lie in their conversion to the $\Delta\rho_N$ values. However, eqs 4a−c (or eq 2) offer no opportunity for making adaptations other than an adjustment of g_{av}^2 (≈5.13) down to $g_e^2 \approx 4$.[62] On the computational side, a provisional scaling factor of ≈0.83 might be applied to the $\Delta\rho_{DFT}$ data, so that these could be used for calculating approximate ϑ^{CON} values in a reversed procedure via eqs 4a−c. Of course, the introduction of either of these global correction factors would improve the overall correlation but not the individual disagreements. It was reassuring to find that the DFT method correctly predicted essentially zero spin densities at several types of H^{ϵ} nuclei (entries S1.150−S1.153), H^{ζ} (lines 35 and 36; S1.163 and S1.160), H^{η} (S1.165), H^{ϑ} (S1.166), and H^{ι} (S1.167). Comparison of the $\Delta\rho_{DFT}$ values in Table S1 (Supporting Information) suggests that other basis sets could be helpful in removing the disagreements. It may be recalled that the B3LYP method was parametrized for heats of formation, not for spin densities, so that $\Delta\rho_{DFT}$ and $\Delta\rho_N$ can be considered to concur reasonably well.

***N*-Aryl Rotation with Chemical Shift Nonequivalence.** For all non-orthogonal chelate/*N*-aryl interplanar angles ($\varphi \neq 90°$), the pairs of ortho and meta positions at the *N*-aryl groups in **6**−**10** are spatially nonequivalent, being nearer (n) to or more distant (d) from the central metal ion. The conformational groundstates have $\varphi = 44-62°$ in the solid[5,6] bis(chelates) **2**, **3a**, and **3b**, while 1,3-dimethyl groups (as in **14**−**16**) are known[8] to tolerate $\varphi = 57-85°$ in the solid state, whereas φ was not specified[63] for 1,3-di-*tert*-butyl substitution. Indeed, our single-point DFT calculations based on the solid-state chelate geometry indicated the $\varphi = 90°$ *N*-aryl conformation to be energetically higher and the 0° orientation to be much higher than the chiral $\varphi = 45°$ conformation, which was then adopted for further quantum chemical calculations and for the estimation of polar coordinates in the previous anisotropy section. Examples of the appertaining geometry factors and ϑ^{MPC} values and their averaging have been deposited in the Supporting Information in Table S2 (entries S2.12−S2.14 and S2.22−S2.24), and Table S1 contains the corresponding $\Delta\rho_{DFT}$ averages.

However, the above nonequivalence (diastereotopism) did not appear even at the lowest temperatures in the ^1H and ^{13}C NMR spectra of the effectively achiral bis(chelates) **1** with $R^1 = R^3$ (if devoid of chiral substitutents). Therefore, the diastereotopic nuclei (ortho/ortho′, or meta/meta′) seem to interchange their environments pairwise at rates of *N*-aryl torsion that are always fast on the NMR time scale. These torsional motions should most easily pass through the $\varphi = 90°$ conformation, corresponding to a time-averaged topology that is depicted in the projection formula **32** (Chart 6), viewed along the *z*-axis C^2-Ni-C^2 (that is, from top to bottom in formula **1Ni**). The two chelate planes appear as crossing horizontal and vertical bars R^3—R^1 in **32a** (chelate twist angle 90°), while the shorter peripheral bars (*a*−*b* and *c*−*d*) symbolize the planes of the four *N*-phenyl groups (drawn at $\varphi = 90°$). For $R^1 = R^3 =$ *tert*-butyl (*t*-Bu, in **19**) or CH_3 (**15**, **23**, or **28**) or H (**9** and **11**−**13**), the effective D_{2d} symmetry postulated in the Introduction is obvious from this model (**32a**) because of the equivalence of all eight ortho or all eight meta positions (single resonance $a + b + c + d$ in either case).

With $R^3 =$ *t*-Bu but $R^1 =$ H in **20Ni**, the symmetry is reduced to C_2 (the diagonal axis) in **32b**, which predicts up to four diastereotopic sites (protons *a*−*d*). Three *N*-*o*-H

(59) Neese, F. *J. Chem. Phys*. **2001**, *115*, 11080−11096.
(60) Zellner, A.; Strassner, T. *Organometallics* **2002**, *21*, 4950−4954.
(61) Frisch, M. J. et al., Gaussian, Inc.: Pittsburgh PA.[26]
(62) Mao, J.; Zhang, Y.; Oldfield, E. *J. Am. Chem. Soc.* **2002**, *124*, 13911−13920.
(63) (a) Budzelaar, P. H. M.; van Oort, A. B.; Orpen, A. G. *Eur. J. Inorg. Chem.* **1998**, 1485−1494. (b) Smith, J. M.; Lachicotte, R. J.; Holland, P. L. *J. Chem. Soc., Chem. Commun.* **2001**, 1542−1543. (c) Eckert, N. A.; Smith, J. M.; Lachicotte, R. J.; Holland, P. L. *Inorg. Chem.* **2004**, *43*, 3306−3321, with extensive applications.

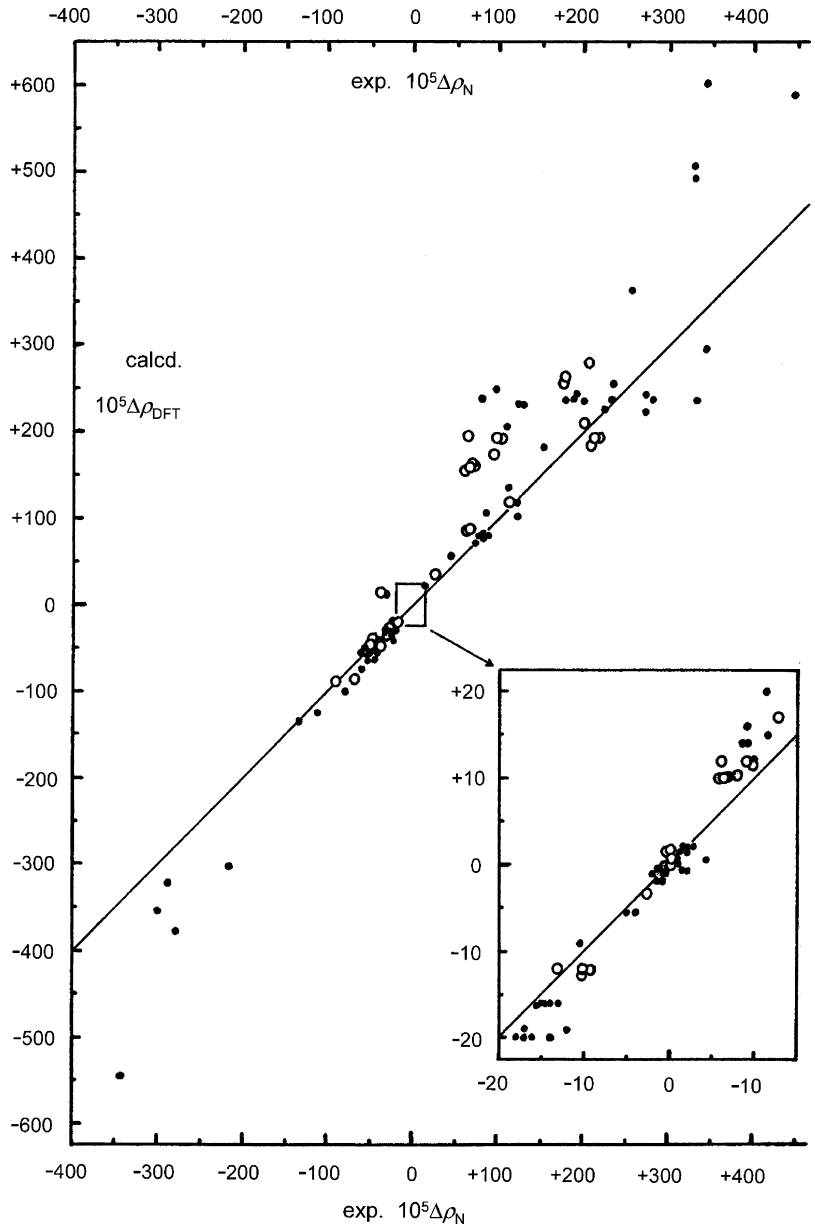

Figure 4. Distribution of ^{1}H and ^{13}C experimental ($\Delta\rho_N$) and computed spin densities ($\Delta\rho_{DFT}$ from UB3LYP/6-311G(d,p)) about the desired 1:1 correlation line. Key: Open circles for **1Co** and filled symbols for **1Ni**. (Enlarged version in the Supporting Information.)

Chart 6

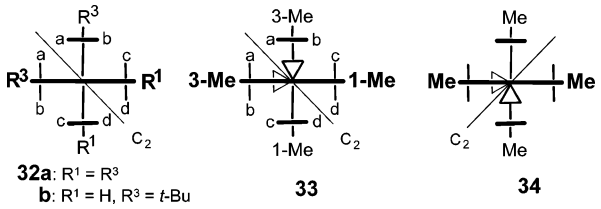

resonances were observed at below +58 °C with the intensity distribution a:b:(c + d) = 2:2:4; these can be assigned unequivocally from Table S36 (Supporting Information) where the chemical shifts of "$a-b$" resemble those of **19Ni** (with $R^3 = R^1 =$ *t*-Bu, Table S34) whereas those of "$c-d$" resemble "normal" ($R^3 = R^1 =$ H) δ^{OBS} values. This suggests analogous assignments for the more closely spaced *N*-*m*-H resonances of **20Ni** with the same splitting pattern a:b:(c + d) = 2:2:4. Clearly, *N*-phenyl rotation of the $a-b$ group adjacent to $R^3 =$ *t*-Bu is slow on the NMR time scale at and below +58 °C. But is it reasonable to ascribe the observed diastereotopic *a*/*b* splitting ($\Delta\delta^{OBS}$ up to 2 ppm in Table S36) to an interaction with the rather remote substituent pair $R^3 \neq R^1$ in the opposing chelate ring? The answer is in the affirmative: The polar coordinates and hence the ϑ^{MPC} values of positions $a-d$ are all equal in **32b**, so that it suffices to calculate only $\Delta\rho_{DFT}$ values. These correspond (by way of eq 4c) to $\Delta\vartheta^{CON}(a-b) \approx 6$ ppm (*o*-H) and ≈ 4 ppm (*m*-H), while $\Delta\vartheta^{CON}(c-d) \approx 0$ was computed for both *o*-H and *m*-H in the less-congested positions. Hence, the observed shift equivalence ($c = d$) for the *N*-phenyl group flanked by R^1 = H does not yet prove fast *N*-phenyl rotation but could also be attributed to a vanishing shift difference.

At above +90 °C, *N*-*o*-H and *N*-*m*-H of **20Ni** were both observed with the changed splitting pattern (a + b):(c + d) = 4:4, caused by an *a*/*b* environmental interchange process

which had now become fast on the NMR time scale. This process must be *N-phenyl rotation adjacent to* R^3 = *t-Bu*, passing through the sterically congested $\varphi = 0°$ conformation: Because of its observed free activation energy $\Delta G^{\ddagger}$(+74 °C) ≈ 17.0 ± 1.5 kcal/mol, it cannot occur by the mechanistic alternative with $\Delta G^{\ddagger} \geq 23.8$ kcal/mol[23] for the Ni configurational inversion (which may consist in 180° rotations of the front (or the rear) chelate ligand as a whole in **32**). Given this rotational barrier toward *N*-phenyl rotation past R^3 = *t*-Bu, it can be inferred that the barrier should be lower for *N*-phenyl rotating past $R^3 = CH_3$ and much lower[26] past R^3 = H.

The time-averaged low-temperature situation in complex **29Ni** ($R^3 = R^1 = CH_3$) is depicted as an axially chiral model in **33**, where the perpendicular orientation of the front substituent R^2 = 1-naphthyl is symbolized as a wedge above its horizontal chelate ring. The wedge pointing to the left in the back belongs to R^2 at the rear (vertical) chelate ligand. At below −18 °C,[64] the *N-m*-H resonances exhibited the narrowly spaced splitting pattern 2:2:4 which could not be assigned because the $\Delta\rho_{DFT}$ values calculated for *N-m*-H with $\varphi = 45°$ (and also for the poorly resolved, very broad *N-o*-H) depend imperceptibly on the 1-naphthyl orientation. Nevertheless, the 4:4 pattern observed at above +5 °C and up to at least +63 °C can be explained as (*a* + *b*):(*c* + *d*) with *fast N-phenyl rotation* of both kinds *of phenyl groups adjacent to* $R^1 = R^3$ = *Me*, interchanging *a* with *b* (or *c* with *d*) in **33** by 180° jumps. At the coalescence temperature (−6 °C), a free energy barrier $\Delta G^{\ddagger}$(−6 °C) ≈ 13.1 ± 0.6 kcal/mol[64] was determined for the slower of these two events. At +104 °C, the two *N-m*-H resonances seemed to have merged to a singlet, but a closer analysis was thwarted by the rapid decomposition of **29Ni**; with $\Delta G^{\ddagger} > 18$ kcal/mol, such a final diastereotopomerization (*a* + *b* interchanged with *c* + *d*) would be attributable to the enantiomerization of **33** to give the antipode **34** and should be caused by Ni configurational inversion rather than by C^2-naphthyl rotation.[65] Neither the 3-Me/1-Me pair of **29Ni** nor the corresponding two kinds of *N-p*-H showed a corresponding diastereotopic signal splitting (expected from **33**) at any chosen temperature, in accord with the tiny calculated $\Delta\rho_{DFT}$ differences of 10^{-7} and 1.5×10^{-7}, respectively.

The computational (DFT) variation of the chelate/*N*-phenyl interplanar angle φ from 0° (full π conjugation) via 45° to 90° (nonconjugation) gave surprising results: The spin density magnitudes $|\Delta\rho_{DFT}|$ at *N-p*-H and several other positions were calculated to *increase* significantly rather than to decrease (Table S3b, Supporting Information). Thus it appears that the gradual π deconjugation might have been overcompensated by a growing $\sigma-\pi$ interaction of the *N*-phenyl π system with some source of σ spin density.

Conclusions

(i) The known technique[39−42] of measuring the ^{2}H NMR signal splitting caused by deuterium quadrupole coupling has furnished magnetic susceptibility anisotropies $\Delta\chi$ of **4Co** and **4Ni** in solution, providing reliable values of metal-centered pseudocontact NMR shifts δ^{MPC} for nuclei at well-defined molecular positions. While this method does not guarantee a successful analysis in situations[41] with lower symmetry, we were able to establish a hyper-Curie[38] temperature dependence of the $\Delta\chi$ values and to deduce that $-\delta^{MPC}$(Ni) amounts to 67% of δ^{MPC}(Co). Such a knowledge of δ^{MPC} opened the path toward the first experimental determinations (by NMR)[66] of unpaired spin densities $\Delta\rho_N$ at magnetically active nuclei of a host of suitable pseudotetrahedral bis(*N*,*N*′-chelates) **1Co** and **1Ni**.

(ii) For nuclei carrying temperature-independent spin densities $\Delta\rho_N$ (the best analyzable type), the Fermi contact NMR shifts δ^{CON} exhibit Curie-type (1/*T*) behavior, so that the "reduced contact shifts" ϑ^{CON} (eq 3) are a most convenient means for determining "experimental" Δ_N values (based on eqs 2 and 4). Owing to the successful separation of δ^{CON} from δ^{MPC}, the bis(chelates) **1** have become a suitable tool for NMR studies of the distribution of unpaired electron spin in organic ligands. In contrast to electron spin resonance measurements with free radicals in general[67] or with a bis(*N*,*O*-chelate)[68] of type **5**, the NMR method provides the signs of $\Delta\rho_N$ directly and can trace long-range spin transfer in **1Co** and **1Ni** with the very high sensitivities of ≈254 000 and ≈201 000 ppm/(unpaired electron spin), respectively, at 298 K as expressed by the corresponding reciprocal factors of $\approx 4 \times 10^{-6}$ and $\approx 5 \times 10^{-6}$ in eqs 4b and c. In addition to this difference, the magnitudes of both $\Delta\rho_N$ and $\Delta\rho_{DFT}$ are regularly smaller for **1Co** than for **1Ni**.

(iii) The chelate ring atom C^2 is situated on the unique magnetic axis ($M-C^2-C^{\alpha}$) and may be regarded as a secondary source of temperature-insensitive spin density that acts as a *small* perturbation on a substituent attached at C^2, so that the spin distribution in such a "downscaled radical" fragment can be interpreted in a transparent way. The pseudocontact NMR shift contributions δ^{MPC} are not modified by rigid rotation about the magnetic axis, as far as the polar coordinates (*R* and θ in eq 6) of the rotating nuclei do not change. Therefore, the substituents at C^2 should be best suited for studying ϑ^{CON} and the rotational dependence of spin transmission.

(iv) The *N*-aryl groups are much less suitable for investigations of the spin distribution in substituents, considering the conformational uncertainties which entail rather crude estimations of the ϑ^{MPC} contributions. Their roughly estimated diastereotopomerization barriers have led to a consistent picture of the modest inhibition of *N*-aryl rotation by vicinal substituents (R^3 = H, CH_3, or *t*-Bu).

(64) The deviating numbers reported previously[25] were based on a misinterpretation in the case of **29Ni** alone and are corrected herewith.
(65) For 1-naphthyl rotation, see: Katz, H. E. *J. Org. Chem.* **1987**, *52*, 3932−3934.
(66) A recently communicated alternative method determined the solid-state pseudocontact shift contributions through single-crystal ^{1}H and ^{14}N ENDOR and NMR measurements: Zhang, Y.; Sun, H.; Oldfield, E. *J. Am. Chem. Soc.* **2005**, *127*, 3652−3653.
(67) Walker, F. A. *Inorg. Chem.* **2003**, *42*, 4526−4544, on p 4533.
(68) Maki, A. H.; McGarvey, B. R. *J. Chem. Phys.* **1958**, *29*, 35−38.

(v) Ligand-centered pseudocontact NMR shifts δ^{LPC} are apparently too small for an unequivocal quantification, perhaps due to the relatively low $\Delta\chi$ values of **1Co** and **1Ni**.

(vi) DFT calculations on the individual bis(chelates) of type **1** furnished theoretical spin densities $\Delta\rho_{DFT}$ that reproduced the trends and most of the signs found experimentally (Figure 4) with a multitude of nuclei. Therefore, they appear to be suitable for corroborating or disproving assignments and interpretations of the NMR contact shifts of this type of complexes.

Experimental Section

The bis(chelates) **4** and **6**−**29** were obtained from their vinamidine ligands by the apropriate (protic or aprotic) known methods, as documented in the Supporting Information, which also contains all other experimental details. Special procedures were used for the following precursors. The 2-(C_6D_5)−malonaldehyde ancestor of the deuterated vinamidine **4H** was prepared[26] from toluene-d_8 via first $C_6D_5-CD_2-CO_2H$ and then two successive iminomethylations[69,70] passing through the morpholino enamine $C_6D_5-CH{=}CH-N(CH_2-CH_2)_2O$. The precursor of vinamidine **13H**, 2-(4-methyl-1-bicyclo[2.2.2]octyl)malonaldehyde, was prepared[26] in a similar manner. The vinamidines **25H** and **27H** (and also the rest of **19H**−**29H** with deconjugated 2-aryl rings) were obtained[26] by C^2-C^3 (rather than C−N) bond formation.[63,71]

Acknowledgment. This work is dedicated to Dr. Hans-Ulrich Wagner in recognition of his long-standing, unabating consultative support. R.K. is indebted to Prof. Bruce R. McGarvey for his explicit calculations,[22] to Prof. F. Ann Walker for her encouragement and enlightening discussions, and to Prof. Hendrik Zipse for efficacious introductions to the computational techniques, followed by much helpful advice. This work was supported by the Deutsche Forschungsgemeinschaft and the Stiftung Volkswagenwerk. The Leibniz-Rechenzentrum der Bayerischen Akademie der Wissenschaften has contributed by the generous allocation of computer time.

Supporting Information Available: Table S1 (δ^{MPC}, ϑ^{CON}, $\Delta\rho_N$, and $\Delta\rho_{DFT}$); Figures S1−S4 (ϑ^{CON}) and Tables S4−S46 (δ^{OBS}, δ^{DIA}, δ^{PARA}, δ^{MPC}, ϑ^{CON} for **6**−**29**) at varied temperatures; measurement of $\Delta\chi$ in detail; derivation of eqs 2, 4, 7, 9, and 10; DFT computational techniques and results; topological averaging; *N*-aryl rotation in **7Ni** and **8Ni**; preparation and characterization of compounds **4**, **6**−**29**, **S36**, **S39**, **S41**, **S44**, **S45**, **S47**, **S48**, a novel dilactone acetal (**S55**), the new azine of ketone **S60**, and some parent substances (**S56**−**S61**). This material is available free of charge via the Internet at http://pubs.acs.org.

IC700656R

(69) Knorr, R.; Löw, P.; Hassel, P. *Synthesis* **1983**, 785−786.
(70) Knorr, R.; Löw, P.; Hassel, P.; Bronberger, H. *J. Org. Chem.* **1984**, *49*, 1288−1290.
(71) Knorr, R.; Weiss, A. *Chem. Ber.* **1982**, *115*, 139−160.